INTERNATIONAL ATOMIC ENERGY AGENCY
UNITED NATIONS EDUCATIONAL, SCIENTIFIC AND CULTURAL ORGANIZATION

INTERNATIONAL CENTRE FOR THEORETICAL PHYSICS
34100 TRIESTE (ITALY) - P.O.B. 586 - MIRAMARE - STRADA COSTIERA 11 - TELEPHONE: 2240-1
CABLE: CENTRATOM - TELEX 460392 - 1

H4.SMR/303 -13

WORKSHOP
GLOBAL GEOPHYSICAL INFORMATICS WITH APPLICATIONS TO RESEARCH IN EARTHQUAKE PREDICTIONS AND REDUCTION OF SEISMIC RISK

(15 November - 16 December 1988)

SOURCE PARAMETERS FROM SHALLOW EVENTS IN THE ROCKY MOUNTAIN HOUSE EARTHQUAKE SWARM

E. NYLAND

University of Alberta
Dept. of Physics
Edmonton T6G 2J1
Canada

Reprinted from

Canadian Journal of Earth Sciences

Source parameters from shallow events in the Rocky Mountain House earthquake swarm

C. J. Rebollar, E. R. Kanasewich, and E. Nyland

Volume 19 • Number 5 • 1982

Pages 907–918

National Research Council Canada / Conseil national de recherches Canada

Réimpression du

Journal canadien des sciences de la terre

Canada

Source parameters from shallow events in the Rocky Mountain House earthquake swarm

C. J. Rebollar

Institute of Earth and Planetary Physics, Department of Physics, University of Alberta, Edmonton, Alta., Canada T6G 2J1 and Centro de Investigación Científica y de Educación Superior de Ensenada, Apdo. Postal 2732, Ensenada, B.C., México

AND

E. R. Kanasewich and E. Nyland

Institute of Earth and Planetary Physics, Department of Physics, University of Alberta, Edmonton, Alta., Canada T6G 2J1

Received September 14, 1981
Revision accepted December 16, 1981

We report here source parameters of the Rocky Mountain earthquake swarm derived from three-component digital dat During 6 days in October 1980, 21 events were recorded. Focal depths for these events are in the range of 1 ± 0.8 to 2 ± 2 km Eleven events with local magnitudes from 2.1 to 2.8 yielded source parameters. Corner frequencies of the *S*-wave spectra we found in the range 6.2 ± 0.5 Hz, giving source dimensions of 160 ± 10 m. The corresponding *P*-wave corner frequencies are the range 8.6 ± 3 Hz. The ratio of *P* to *S* corner frequencies varies from 0.9 to 2.1. There is a path effect between 13 and 16 H that could have affected these ratios. The average falloff over three components at high frequencies varies from −1.8 to −2. High stress drops, ranging from 47 to 263 bar (4.7–26.3 MPa), and apparent stresses, from 2.5 to 23 bar (0.25–2.3 MPa), we calculated. Five events have remarkably similar characteristics in the frequency and time domains. For these events the ratio minimum strain energy W_0, according to Kanamori, to the energy calculated using the integration scheme of Hanks and Thatch was 3.7 ± 0.5. A theoretical value gives 3.1. The seismic efficiency ranges from 0.2 ± 0.04 to 0.17 ± 0.8. Large seism moments for relatively small magnitudes were found. Some of these spectral characteristics are best explained as the result displacement along a smooth fault.

Nous rapportons ici les paramètres de la source sismique d'une série de tremblements de terre dans les Montagnes Rocheus dérivés à l'aide de données numériques de trois composantes. En octobre 1980, 21 secousses sismiques ont été enregistrées en jours. Les profondeurs des épicentres pour ces secousses sismiques varient entre 1 ± 0,8 et 2 ± 2 km. Onze secousses sismiqu avec des magnitudes locales de 2,1 à 2,8 ont fourni les paramètres de la source. Les fréquences au coude des ondes-*S* du spect fournissent une valeur de 6,2 ± 0,5 Hz, ce qui donne comme dimensions de la source 160 ± 10 m. Les fréquences au coude d ondes-*P* sont de 8,6 ± 3 Hz. Le rapport des fréquences au coude des ondes varie de 0,9 à 2,1. Il existe un effet dû au cheminem des ondes entre 13 et 16 Hz qui peut avoir modifié ces rapports. Le ralentissement moyen pour les trois composantes à haut fréquences varie de −1,8 à −2,3. Les fortes chutes des contraintes dans le domaine de 47 à 263 bar (4,7–26,3 MPa) et l contraintes apparentes de 2,5 à 23 bar (0,25–2,3 MPa) furent calculées. Cinq secousses sismiques présentent des caractéristiqu similaires en fréquence et en durée. Pour ces secousses sismiques le rapport de l'énergie minimum de tension W_0, définie p Kanamorie, et de l'énergie calculée au moyen de la méthode d'intégration de Hanks et Thatcher était de 3,7 ± 0,5. Un cal théorique donne 3,1. L'efficacité sismique varie de 0,2 ± 0,04 à 0,17 ± 0,8. On observe des moments sismiques élevés pour c magnitudes relativement petites. Certaines de ces caractéristiques spectrales s'expliquent plus clairement par un mouvement long d'un plan uni de faille.

[Traduit par le journ

Can. J. Earth Sci., 19, 907–918 (1982)

Introduction

During late September and early October of 1980, a local array of five analog vertical portable seismic stations was operated by R. J. Wetmiller of the Division of Seismology and Geothermal Studies of the Earth Physics Branch, Canada Department of Energy, Mines and Resources. One University of Alberta digital three-component portable station was deployed near Rocky Mountain House, Alberta in order to study the seismicity of the area. This area is the most active zone of seismicity in the Foothills. Some of this activity has been detected at Edmonton (Rebollar *et al.* 1982).

Events recorded by the analog and digital instruments were confined to an area of approximately 8 km^2 near 52°12′N and 115°14′W at a depth of 4 ± 2 km (Fig. Wetmiller 1981). Those events may be confined to hydrocarbon-bearing sedimentary layer in upper P eozoic strata.

This study is mainly concerned with the evaluation focal depths and source parameters with a genera accepted source model (Brune 1970, 1971). The source parameters are compared with already publish data, theoretical models, and results from laborat experiments of shear crack displacements, in a effort explain their particular features.

Digital recorder

A three-channel Sprengnether digital recording s

0008-4077/82/050907-12$01.00/0

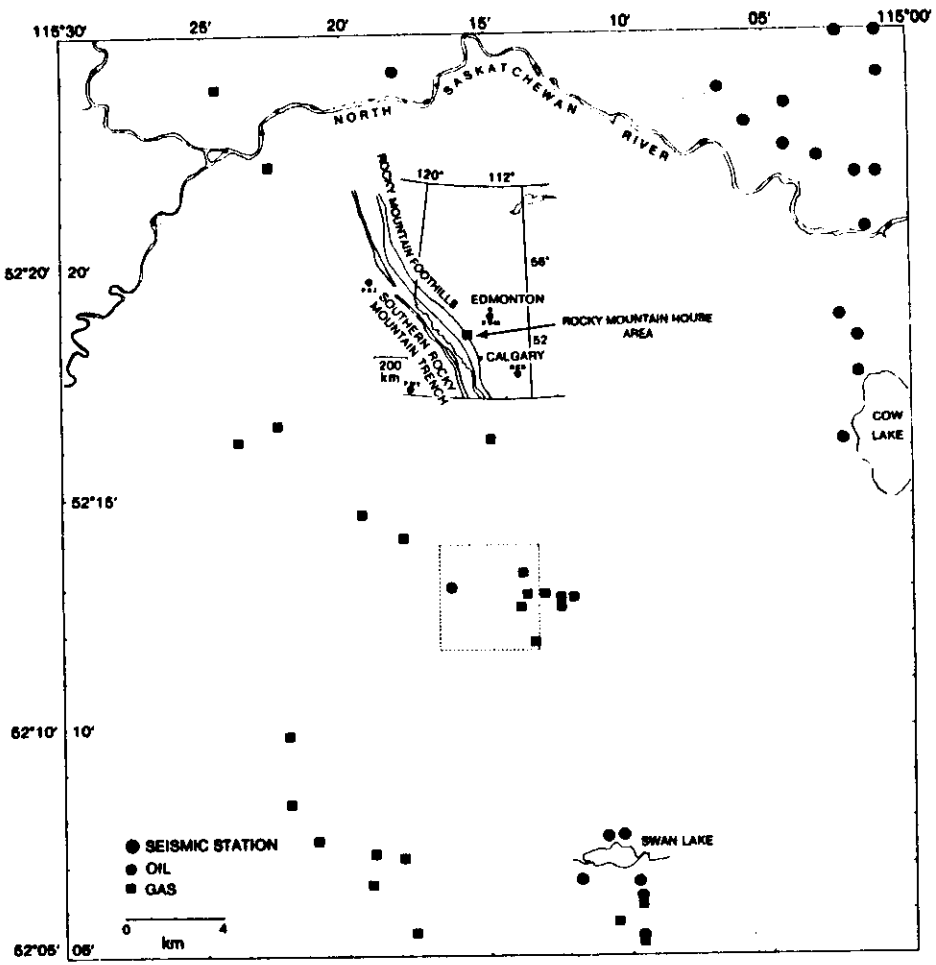

FIG. 1. The location of the Rocky Mountain earthquake swarm. The dashed lines isolate the seismic locations reported by 'etmiller (1981) and the location of the digital seismic station. Almost all locations were near the gas wells.

m model DR-100 was used in this experiment. This cording system was connected to five-pole antialiasing utterworth filters and to Mark product L-4C 1.0 Hz ismometers, to provide a single three-component rtable station. The sampling rate used in this experient was 100 samples/s. Absolute time was synchrozed with the WWVB signal. A response curve for the mbined recorder–seismometer for maximum gain of 0 and 60 dB is given in Fig. 2. The station was located 52.23°N and 115.27°W, southwest of Rocky Mountin House, and operated from October 3 to October 9, 1980 (Fig. 1). The station was set up in sediments from the Cretaceous, and operated with a gain of 66 dB due to local background noise (mainly wind-generated and oilfield activity).

Event locations

In order to analyse the events we need a structural model. Richards and Walker (1959), from an approximately north–south refraction profile near 113.5°W and between 50.8°N and 51.9°N, reported two sedimentary layers above the basement. The upper one is of

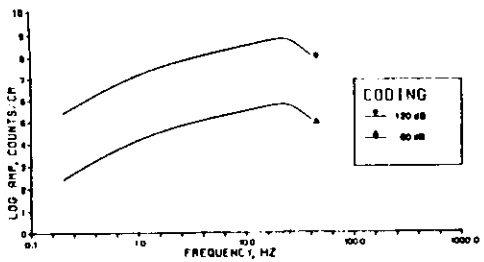

FIG. 2. Magnification curves of the digital station at 20 and 120 dB. The station was operated at 66 dB.

Mesozoic age with a thickness of 2 km and a P velocity of 3.6 km/s. The lower one is from the Paleozoic with a thickness of 1.5 km and a P velocity of 6.1 km/s. One of these events shows no discernible P or S waves. Five events are remarkably similar in all three components (bottoms of Figs. 4 and 5). This is not the first time that this kind of earthquake has been observed. Geller and Mueller (1980) reported four similar earthquakes in central California at epicentral distances of 20–51 km. This also has been observed in the Victoria earthquake swarm of 1978 in the valley of Mexicali, Mexico and in the aftershocks of the Oaxaca earthquake of November 28, 1978 (L. Munguia, personal communication, 1979). This similarity implies that they are clustered in space so that they follow the same path to the recording station. The maximum amplitude was recorded in the east–west component, where there was a dominant signal with a period of about 0.2 s that corresponded to a wavelength of 0.6 km, assuming an S-phase velocity of 3.0 km/s.

The $S-P$ times of these events were in the range 1.0 ± 0.4 s. The P arrival was read in the vertical component and the S arrival in the horizontal component. We calculated theoretical travel-time curves using the Richards and Walker (1959) model. A travel-time curve for a source depth of 2 km gives an epicentral distance of 3 km, for a source depth of 4 km. This corresponds to an epicentral distance of 2.65 km. Deeper source depths do not predict the observed $S-P$ time; for example, a travel-time curve for a source depth of 6 km predicts a minimum $S-P$ time of 1.2 s above the epicenter. Therefore these events have a source depth of approximately 2 ± 2 km (Fig. 3*a*).

These events do not have a large content of high frequencies, even though the station was very near the epicenter. It is well known that irregular rupture dislocations with variable slip and complex strength on the fault enhance high-frequency waves (Miyatake 1980*a*,*b*). Perhaps these events correspond to a process in which a barrier is being repeatedly broken and healed. In this case the events share the same dynamic and kinematic characteristics. Another possibility is a collinear shear crack (Rudnicki and Kanamori 1981). Geller and Mueller (1980) suggest that the clustering and similarity indicate that these earthquakes can represent stress release at the same asperity.

One event with a relatively large $S-P$ (2.1 s) time was recorded; therefore it is not possible to determine the approximate depth or epicentral distance. We filtered the signal for this event with different bandwidths and still observed clear P and S waves. Perhaps it was one of the deep events that were analysed using S_n phases at Edmonton by Rebollar *et al.* (1982). Unfortunately this event was not recorded at Edmonton (Fig. 3*b*).

Calculation of the spectra

This is the first time that this kind of analysis has been done in the Foothills of the Rocky Mountains at short epicentral distances (less than 5 km). Source characteristics at large epicentral distances, approximately 170 km, for events recorded at station EDM in the Rocky Mountain earthquake swarm were analysed by Rebollar *et al.* (1981).

Source parameters were calculated using Brune's (1970, 1971) model. This theory has been found to be valid both at short epicentral distances of a few kilometres and at teleseismic distances. See, for example, Hanks and Thatcher (1972), Hanks and Wyss (1972), and Hanks (1981) among others in an extensive literature.

Corrections applied before the calculation of seismic moment were: free surface reflection of S_H or S_V waves, radiation pattern, seismic attenuation, geometrical spreading, and instrument response. In this study 11 reliable events were used in order to get source parameters. Epicentral locations, azimuths, and angles of incidence calculated by R. J. Wetmiller (personal communication, 1981) were used. These events were rotated in order to have a "pure" S_H wave in the transverse component, and the horizontal component of the S_V wave in the radial term. Corrections for free surface reflection of the radial and vertical components of S_V waves were calculated using Nuttli's (1961) formulas. Taking into consideration short epicentral distances and the sedimentary layers of the Foothills, a Q of 150 was used to correct for attenuation in both S and P spectra. However, errors in the choice of Q were not critical because of short epicentral distances.

The sedimentary layers of the Foothills consist of shales, siltstones, sandstones, and carbonates with accumulations of hydrocarbons ranging in age from the Cretaceous Period to the Cambrian Period in the Paleozoic Era (Bokman 1963). Therefore, we assumed a P-wave velocity of 5 km/s, a density of 2.5 g/cm^3, and a Poisson ratio of 0.33, in order to take into considera-

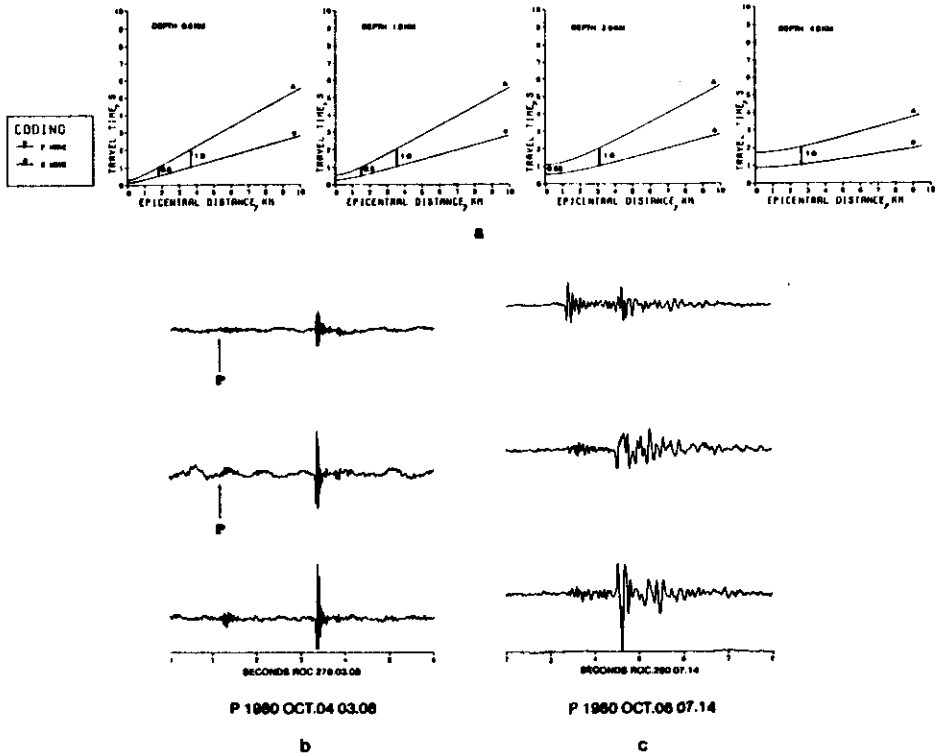

FIG. 3. (*a*) Travel-time curves for different depths using the Richards and Walker (1959) model. Arrows show *S*–*P* times of approximately 1.0 s for typical events. (*b*) Possible deep event. (*c*) Typical event with *S*–*P* time of approximately 1 s.

tion the low-velocity body waves of sediments reported by Richards and Walker (1959). Sample lengths of 1.0 and 1.5 s were used for *S*-wave spectra and 0.5 s for *P*-wave spectra. All the spectra were filtered between 1 and 45 Hz and smoothed with a Daniel window of 1 Hz.

Source parameters and discussion of the spectra

Eighteen events with *S*–*P* times of the order of 1 s were analysed; of these, 11 yielded source parameters. The spectra of these events show a significant path effect between 13 and 16 Hz in the transverse or north–south component and vertical component of the spectra. This effect is less prominent in the radial or east–west component. This path effect makes it difficult to recognize corner frequencies, and sometimes it suggests a spurious corner frequency of high frequencies (Figs. 4, 5). In the spectra of *P* waves this effect is even more noticeable, moving the corner frequency of four events up to 11 Hz (Fig. 8).

Laboratory experiments have shown that the spectra of waves radiated from the displacement of a homogeneous fault have a simple spectrum, i.e., a low-level amplitude and the falloff at high frequencies with a few peaks decreasing in amplitude. However, displacement spectra from an inhomogeneous fault (with asperities or obstacles) have a different form: the low-level amplitude and the peaks in the falloff at high frequencies are comparable in magnitude with the low-level trend, suggesting two corner frequencies (Vinogradov 1978). Therefore, these results could explain high peaks at "high" frequencies in our spectra. However, the same experiments show that shear displacement along a homogeneous fault (without asperities) gives a high seismic moment for a relatively small magnitude. This is in agreement with our results. Since seismic moment is a

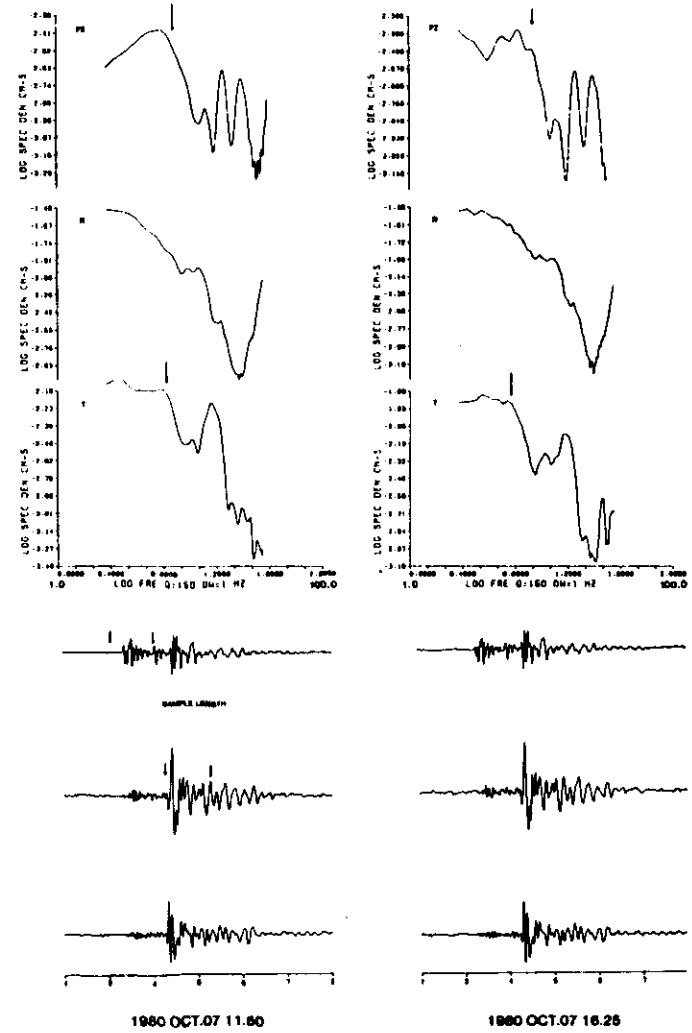

FIG. 4. Similar events and the spectra of the transverse (T) and radial (R) components of the *S* wave. PZ is the *P*-wave spectru calculated from the vertical component. Arrows show the corner frequency and the sample interval used in the evaluation of t spectra (all of the spectra were calculated at 60 dB; therefore they should be decreased by 6 dB in order to get 66 dB).

more reliable parameter we conclude that those effects present in the observed spectra are more likely due to local inhomogeneities.

Corner frequencies were found in the range of 5.8–6.3 Hz (Figs. 6, 7). This is equivalent to source dimensions of 161–148 m. Some corner frequencies the *P*-wave spectra are strongly affected by path effe as can be seen in the spectra of Fig. 8. Hanks (198 pointed out that source parameters calculated at a sing station are more likely to be affected by path effects.

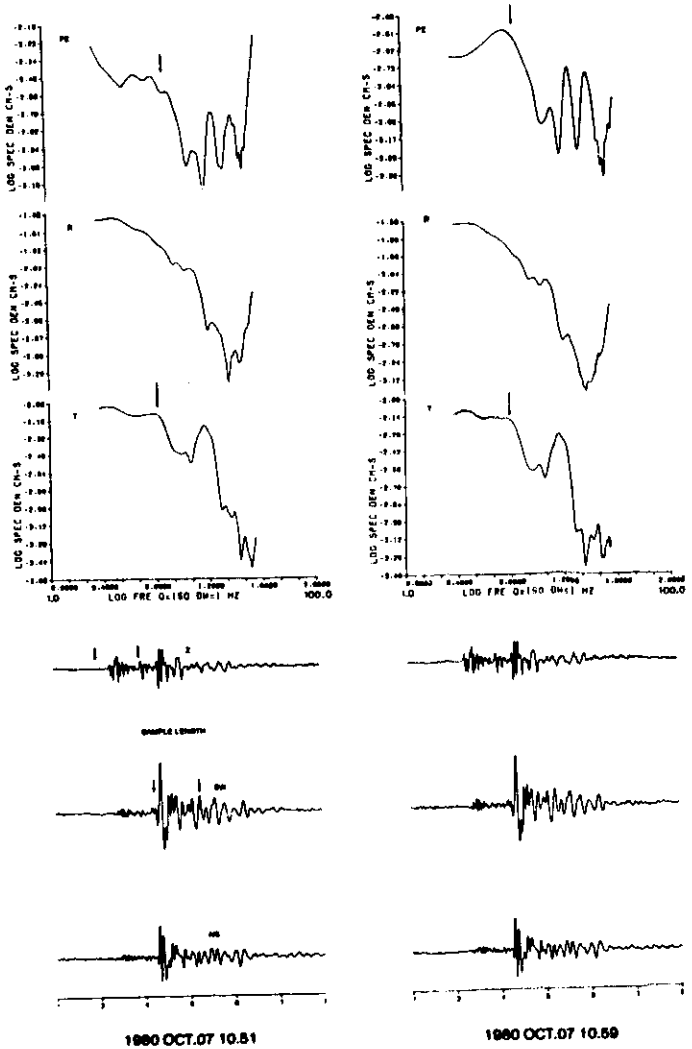

FIG. 5. Similar events and the spectra of the transverse (T) and radial (R) components of the *S* wave. PZ is the *P*-wave spectrum alculated from the vertical component. Arrows show the corner frequency and the sample interval used in the evaluation of the pectra.

Stress drops for those 11 events were consistently igh, ranging from 47 to 263 bar (4.7–26.3 MPa). revious work has found stress drops in the range of a ew tenths of a bar to 100 bar (10 MPa) for events with ocal magnitudes from −1.3 to 3.4 (Wyss and Brune 968; Douglas and Ryall 1972; Thatcher and Hanks 1973; Bakun *et al.* 1976; Johnson and McEvilly 1974; Fletcher 1980; Marion and Long 1980; Rebollar *et al.* 1982).

Bakun *et al.* (1976) reported stress drops of the order of 245 bar (24.5 MPa) calculated from the spectra of *P* waves. Hartzell and Brune (1977) found stress drops in

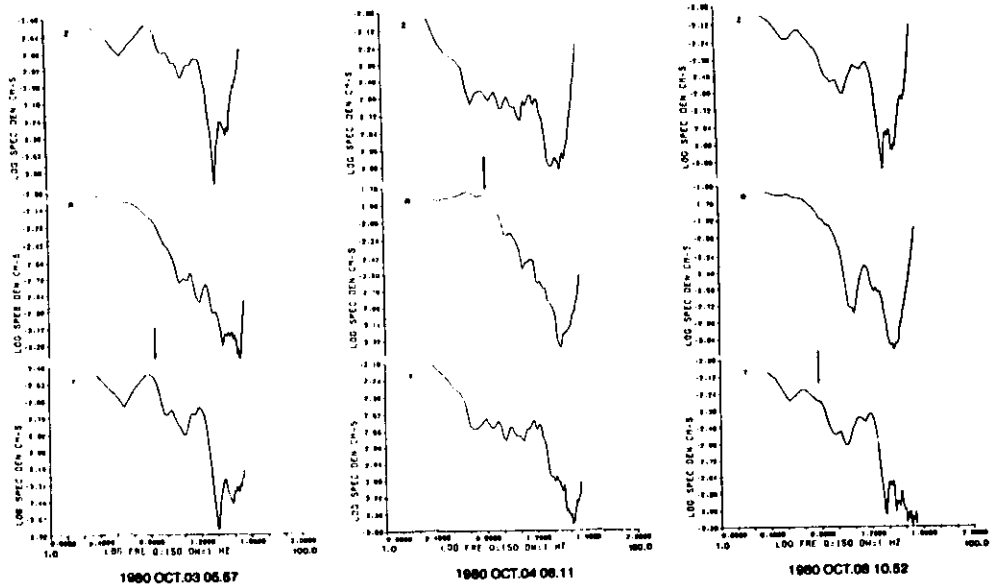

FIG. 6. Spectra of the vertical (Z), radial (R), and transverse (T) components of the *S* wave of the events used in this analysis. Arrows show corner frequencies. Some spectra show possible path inhomogeneities.

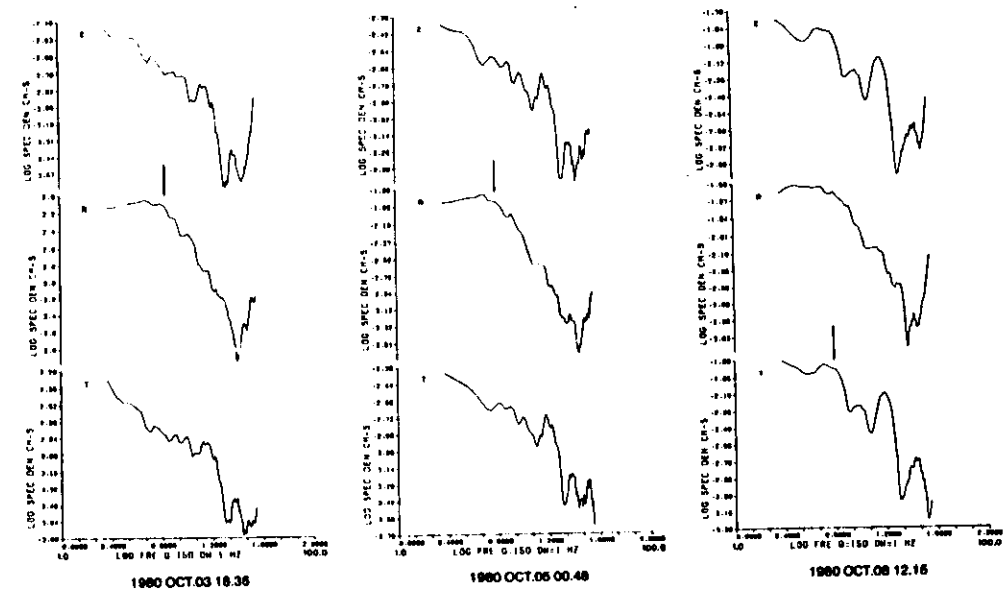

FIG. 7. Spectra of the vertical (Z), radial (R), and transverse (T) components of the *S* wave of the events used in this analysis. Arrows show corner frequencies. Some spectra show possible path inhomogeneities.

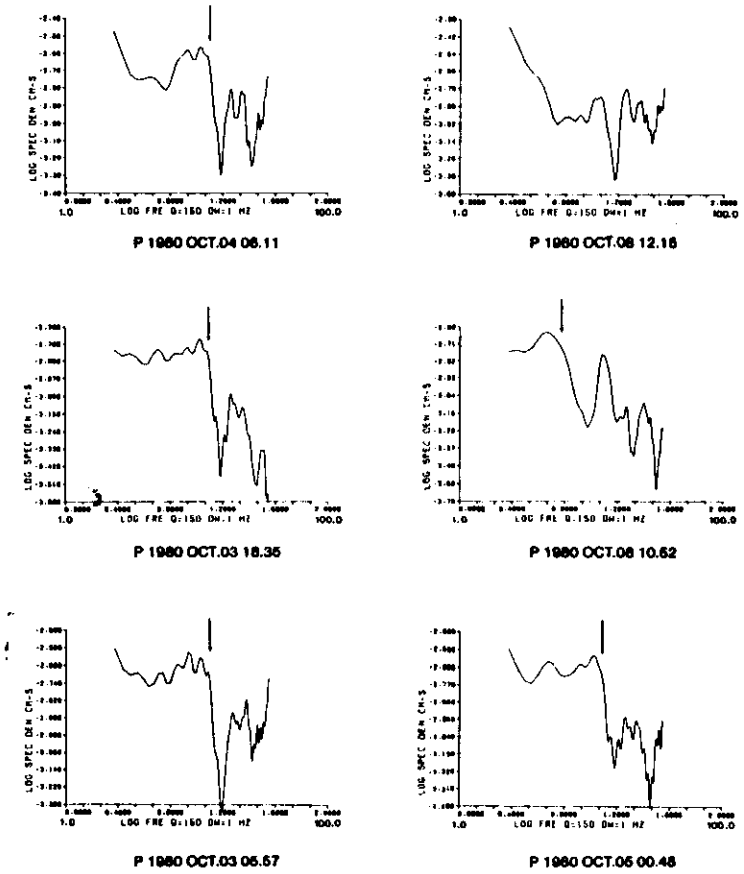

FIG. 8. *P*-wave spectra of the events of Figs. 6 and 7. These events show a possible path effect in the corner frequencies; *P*-wave corner frequencies were usually higher than their respective *S*-wave corner frequencies.

the range of 1–636 bar (0.1–63.6 MPa) for 61 events of the Brawley earthquake swarm with magnitudes from 1 to 4.7.

Stress drops of possible deep events of the Rocky Mountain House earthquake swarm are of the order of a few tenths of a bar (Rebollar *et al.* 1982). Since the shallow events have high stress drops, this seems to contradict the observations that the stress drop increases with depth (Fletcher 1980; Hartzell and Brune 1977). However, this observation could indicate that shallow events are an indirect consequence of the extraction of oil and gas whereas deep events are more likely of tectonic origin. Figure 1 shows the epicentral area reported by Wetmiller (1981). Those epicenters tend to lie near the gas wells of the Strathcona fields.

Source parameters of the five similar events are more homogeneous, reflecting the almost perfect match in the seismograms. A plot of local magnitude versus seismic moment (Fig. 9) shows consistently large seismic moments for this range of magnitudes. However, they follow the same slope as the relation $\log M_0 = 1.3M_L + 16.6$ (Rebollar *et al.* 1982). Large seismic moments for relatively small magnitudes have been observed in laboratory experiments of shear sliding along a smooth fault (Vinogradov 1978). This could explain those high moments, even though laboratory experiments are an oversimplification of a real earthquake.

The radiated energy E was calculated using Hanks and Thatcher's (1972) integration scheme. They found an analytic expression integrating the far-field shear

TABLE 1. Source parameters of selected events

ID	Recording time	M_L	M_0 (dyn·cm)	E_s (erg)	f_S	f_P	f_P/f_S	$\bar{\gamma}$	r (m)	$\Delta\sigma$ (bar)	η	$\eta\sigma$ (bar)	$\Delta\sigma/\eta\bar{\sigma}$	Δ (km)
1	1980 Oct. 03 05.57	2.1	2.68×10^{20}	6.2×10^{15}	6.4	11.6	1.8	1.8	150	47.3	0.15	3.61	13.1	2.0
2	1980 Oct. 03 18.35	2.1	1.47×10^{20}	2.41×10^{15}	6.7	11.6	2.1	2.0	169	62.1	0.08	2.56	24.2	1.0
3	1980 Oct. 04 06.11	2.4	7.07×10^{20}	6.60×10^{16}	6.3	11.4	1.8	2.3	148	211.0	0.14	14.56	14.5	2.0
4	1980 Oct. 05 00.48	2.3	2.21×10^{20}	8.28×10^{15}	6.3	11.3	1.8	2.2	148	74.7	0.16	5.84	12.8	1.0
5	1980 Oct. 08 10.52	2.5	1.15×10^{21}	1.71×10^{17}	5.8	5.5	0.9	1.5	172	142.0	0.33	23.20	6.1	5.0
6	1980 Oct. 08 12.15	2.8	1.56×10^{21}	2.18×10^{17}	6.3	—	—	1.9	150	263.3	0.17	21.80	12.08	3.0
	Similar events													
7	1980 Oct. 07 10.51	2.6	8.28×10^{20}	8.99×10^{16}	6.2	7.4	1.19	2.2	150	113.5	0.30	16.94	6.7	2.0
8	1980 Oct. 07 10.59	2.5	6.70×10^{20}	5.30×10^{16}	6.0	7.1	1.18	2.1	155	92.1	0.27	12.34	7.4	2.0
9	1980 Oct. 07 11.50	2.6	8.28×10^{20}	6.05×10^{16}	5.9	7.1	1.20	1.9	158	105.7	0.22	11.40	9.2	2.0
10	1980 Oct. 07 16.25	2.8	1.15×10^{21}	1.39×10^{17}	5.8	7.3	1.26	2.2	161	146.0	0.26	18.86	7.7	2.0
11	1980 Oct. 08 04.59	2.7	1.04×10^{21}	1.31×10^{17}	5.9	9.1	1.54	2.1	158	127.4	0.31	19.65	6.4	2.0

NOTES: M_L = local magnitude; M_0 = seismic moment (1 dyn = 10 μN); E_s = radiated seismic energy (1 erg = 0.1 μJ); f_S, f_P = *S*-wave, *P*-wave corner frequency; γ = average falloff of the spectra at high frequencies; r = source dimension; $\Delta\sigma$ = stress drop (10 bar = 1 MPa); η = seismic efficiency; $\eta\bar{\sigma}$ = apparent stress (10 bar = 1 MPa); Δ = epicentral distance.

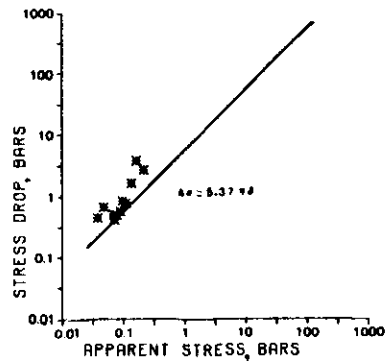

FIG. 9. Plot of apparent stress versus stress drop. The heavy line shows the Hartzell and Brune (1977) relation for the Imperial Valley earthquake swarm. Similar events have a relation to $\Delta\sigma = (7.4 \pm 1.1)\eta\bar{\sigma}$. Events 1–6 have a ratio of 11.9 with a great standard deviation (9.2). Note: 10 bar = 1 MPa.

displacement spectra proposed by Brune (1970), assuming a complete stress drop ($\epsilon = 1$) and a falloff of -2 at high frequencies. Thatcher and Hanks (1972), however, pointed out that uncertainties in the falloff at high frequencies can give a misleading measure of the energy. In our case the average slope in the three components of the shear spectrum at high frequencies varies from 1.8 to 2.3 (Table 1). Therefore, errors in the calculation of the radiated energy due to the slope at high frequencies are small. Most of the energy of small earthquakes is radiated in short-period waves; hence, because of the short epicentral distances, little energy can be lost. Therefore the integration scheme can give a better estimate of the radiated energy.

Energies range from 2.4×10^{15} erg (2.4×10^{8} J) ($M_L = 2.1$) to 2.1×10^{17} erg (2.1×10^{10} J) ($M_L = 2.8$). Radiated seismic energies calculated using Gutenberg and Richter's (1956) and Thatcher and Hanks' (1973) empirical relations derived for California give smaller values as we can see from Fig. 10. This could mean that the integration scheme gives a better estimate of the radiated energy at short epicentral distances (less than 4 km).

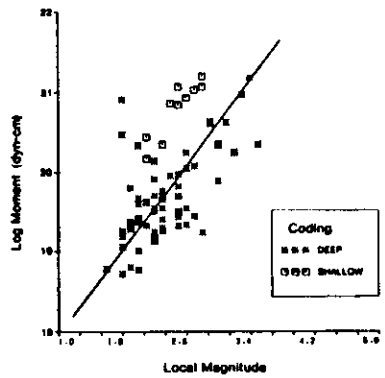

FIG. 10. A comparison of the relation of local magnitude versus seismic moment for deep events detected at the digital station of Edmonton and shallow events recorded with the portable digital station. The heavy line shows the relation $\log M_0 = 1.3M_L + 16.6$ (Rebollar *et al.* 1982). Note: 1 dyn = 10 μN).

Corner frequencies of P-wave spectra were consistently larger than those of the S-wave spectra. Only one corner frequency of P waves was found to be less than the corresponding corner frequency of the S-wave spectra (Table 1). P-wave frequencies seem to be more affected by local path effects. Those path effects are easily recognized because they appear in the same range of frequencies, independent of the obvious variation in the radiation pattern that can be recognized by inspection of the seismograms. Ratios of the P and S frequencies (corner frequency shifts) were found in the range of 0.9–2.1. However, the average ratio of f_P to f_S in similar events is 1.2 ± 0.2, more in agreement with the general observation that f_P/f_S is greater than one and with theoretical models that treat earthquakes as equidimensional faults (Brune 1970; Madariaga 1976; Burridge 1975) or long and narrow faults with near-sonic or transonic rupture velocities (Savage 1974). Hanks (1981) suggests that the frequency shift is an intrinsic characteristic of the far-field spectra of body waves independent of source strength (seismic moment), hypocenter, epicentral distance, or recording device.

The minimum strain energy drop W_0 (Kanamori 1977) is

$$[1] \quad W_0 = (\Delta\sigma/2\mu)M_0$$

which assumes a complete stress drop if $\sigma_2 = 0$ or if the Orowan (1960) condition is met ($\sigma_2 = \sigma_f$). Substituting in [1] the moment and stress drop according to Brune (1970, 1971), we get

$$[2] \quad W_0 = \frac{212\pi}{1.26}\rho\beta R^2\Omega_0^2 f_c^3$$

where ρ is the density; β is the shear-wave velocity; R is the epicentral distance; f_c is the corner frequency; Ω_0 is the low-level amplitude of the S_H spectra; and 1.26 is the product of the average radiation pattern and the free surface reflection of S_H waves. The radiated seismic energy E_s according to the integration scheme of Hanks and Thatcher (1972) is given by

$$E_s = \frac{128\pi^3}{15(1.26)^2}\rho\beta R^2\Omega_0^2 f_c^3$$

Taking the ratio of W_0 and E_s we get $W_0 = 3.1E_s$. If we assume that one third of the seismic energy is contained in the P wave, we have $W_0 = 4.1E_s$. This means that even though W_0 is a minimum estimate of the energy, the integration scheme gives even lower values of the radiated energy. Table 2 gives the values of W_0, E_s, and the ratio W_0/E_s. This ratio for similar events is 3.7 ± 0.5, in good agreement with the theoretical result ($W_0 = 3.1E_s$), which does not include the contribution of the P-wave energy. However, events 1–6 give an average ratio of 6.8 with a large standard deviation of 3.

TABLE 2. Comparison of energy estimates

M_L	Minimum strain energy drop W_0* (erg)	Radiated seismic energy E_s† (erg)	W_0/E_s
2.1	4.1×10^{16}	6.2×10^{15}	6.5
2.1	2.9×10^{16}	2.4×10^{15}	12.2
2.4	4.8×10^{17}	6.6×10^{16}	7.2
2.3	5.3×10^{16}	8.3×10^{15}	6.4
2.5	5.2×10^{17}	1.7×10^{17}	3.0
2.8	1.3×10^{18}	2.2×10^{17}	6.0
	Similar events		
2.6	3.0×10^{17}	8.9×10^{16}	3.3
2.5	1.9×10^{17}	5.3×10^{16}	3.7
2.6	2.8×10^{17}	6.0×10^{16}	4.6
2.8	5.4×10^{17}	1.4×10^{17}	3.8
2.7	4.2×10^{17}	1.3×10^{17}	3.2

NOTES: M_L = local magnitude; 1 erg = 0.1 μJ.
*From Kanamori (1977).
†From Hanks and Thatcher (1972).

The apparent stress is defined (Wyss 1970) as

$$\eta\bar{\sigma} = \mu E_s/M_0$$

where η is the seismic efficiency; $\bar{\sigma}$ is the average shear stress; μ is the shear modulus; E_s is the radiated seismic energy; and M_0 is the seismic moment. Uncertainties in the evaluation of the apparent stress are a direct consequence of the uncertainties in the evaluation of the radiated energy. Therefore the seismic efficiency is one of the most uncertain parameters in seismology. However, Wyss (1970) calculated a seismic efficiency of 0.1 for deep and intermediate earthquakes in South America. Apparent stress calculated by the Wyss formula ranges from 2.5 to 23.2 bar (0.25–2.32 MPa) (Table 1). A plot of stress drop versus apparent stress can be compared with that calculated by Hartzell and Brune (1977). Even though there is some scatter, it follows a similar trend (Fig. 11). Those differences indicate regional variations in the apparent stress and consequently the state of stress in the crust of the Rocky Mountain House area.

The ratio of stress drop to apparent stress for similar events is almost constant at 7.4 with a standard deviation of 1.1. This ratio suggests a possible way to calculate absolute stress; however, in order to do this it is necessary to know the seismic energy and the frictional energy.

Following Wyss (1970) it is possible to calculate an approximate upper bound for the seismic efficiency given by

$$\eta_{max} = 2\eta\bar{\sigma}/\Delta\sigma \geq \eta$$

Seismic efficiency calculated in this way for similar events gives a constant value of 0.2 ± 0.04. This reflects

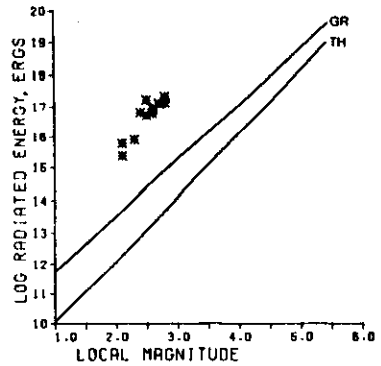

FIG. 11. Plot of local magnitude versus log of radiated seismic energy calculated using the Hanks and Thatcher (1972) integration scheme. For comparison we plotted the Gutenberg and Richter (1956) (GR log $E = 9.9 + 1.9M_L - 0.024M_L^2$) and Thatcher and Hanks (1973) (TH log $E = 2.0M_L + 8.1$) empirical relations for California.

the correct selection of corner frequencies in the spectra. Events 1–6 give 0.17 ± 0.8 (Table 1). These high values apparently suggest a high conversion of potential energy to elastic seismic energy for these shallow earthquakes.

Conclusions

Events with S–P times of about 1 s and source depths of 2 ± 2 km show different amplitudes of P and S waves, indicating dislocations with distinct fault orientations. Similar events have small variations in source parameters, perhaps indicating a process in which a barrier or asperity is being repeatedly broken and healed. Stress drops and apparent stress were consistently high for all the events. Hydrocarbon recovery operations can cause concentration of stresses in surrounding areas. This could result in brittle fracture in the sedimentary rocks or the granitic basement by activating ancient faults and joints or by rupturing along preexisting cracks. Laboratory experiments reveal a lesser accumulation of strain energy, and consequently stresses, in a closed fracture as compared with an open fracture (Shamina *et al.* 1978). Therefore, high stresses could indicate a highly fractured zone, since stress drops represent minimum tectonic stresses related to the seismic events.

Radiated seismic energy calculated using $W_0 = (\Delta\sigma/2\mu)M_0$ (Kanamori 1977; Hanks and Thatcher 1972) gives a ratio of 3.1, in good agreement with the observed ratio of 3.7 ± 0.5 for similar events. Larger energies were obtained for a given magnitude using the Hanks and Thatcher (1972) method than for those calculated using the empirical relationships of Gutenberg and Richter (1956) and Thatcher and Hanks (1973) for events in California. This could mean that the integration scheme gives a better estimate of the radiated energy at short epicentral distances (less than 4 km). Values of 0.2 ± 0.04 and 0.17 ± 0.8 for the seismic efficiency were found, suggesting a high conversion of potential energy to elastic energy for these shallow earthquakes.

Corner frequencies of the S-wave spectra were found between 5.8 and 6.7 Hz, giving source dimensions of 150–169 m. The ratio of corner frequencies of P-wave and S-wave spectra gives a value of 1.2 ± 0.2 for similar events, as has been usually observed (Hanks 1981). However, corner frequencies for events 1–6 give ratios ranging from 0.9 to 2.1. These ratios could have been effected for local inhomogeneities, such as that found in our spectra between 13 and 16 Hz.

A plot of local magnitude versus seismic moment gives systematically large seismic moments for relatively small magnitudes. This follows the same trend as the relationship found for deep events by Rebollar *et al.* (1982). Laboratory experiments show that displacement along a smooth fault is a possible mechanism of earthquakes with large seismic moments and a relatively small magnitude (Vinogradov 1978). This could explain those high moments.

Acknowledgements

We would like to thank Bruce McGavin and Panos Kelamis who did the field work for this study. We also appreciate the invaluable assistance of Charlie McCloughan in helping to process the digital data. One of us (CJR) was supported by El Consejo Nacional de Ciencia y Tecnologia de Mexico (CONACYT). This research was supported by funds from the Natural Sciences and Engineering Research Council of Canada. We appreciate the cooperation of R. J. Wetmiller and the Earth Physics Branch, Department of Energy, Mines and Resources, Ottawa.

BAKUN, W. H., BUFE, C. G., and STEWART, R. M. 1976. Body-wave spectra of central California earthquakes. Bulletin of the Seismological Society of America, 66, pp. 363–384.

BOKMAN, J. 1963. Post-Mississippian unconformity in western Canada basin. *In* Backbone of the Americas. *Edited by* O. E. Childs. American Association of Petroleum Geologists, Memoir 2, pp. 231–242.

BRUNE, J. N. 1970. Tectonic stress and the spectra of seismic shear waves from earthquakes. Journal of Geophysical Research, 75, pp. 4997–5009.

——— 1971. Correction. Journal of Geophysical Research, 76, p. 5002.

BURRIDGE, R. 1975. The effect of sonic rupture velocity on the ratio of S to P corner frequencies. Bulletin of the Seismological Society of America, 65, pp. 667–675.

DOUGLAS, B. M., and RYALL, A. 1972. Spectral characteris-

tics and stress drop for microearthquakes near Fairview Peak, Nevada. Journal of Geophysical Research, **77**, pp. 351–359.

FLETCHER, J. B. 1980. Spectra from high-dynamic range digital recordings of Oroville, California aftershocks and their source parameters. Bulletin of the Seismological Society of America, **70**, pp. 735–755.

GELLER, J. R., and MUELLER, C. S. 1980. Four similar earthquakes in central California. Geophysical Research Letters, **7**, pp. 821–824.

GUTENBERG, B., and RICHTER, C. F. 1956. Earthquake magnitude, intensity, energy, and acceleration. Bulletin of the Seismological Society of America, **46**, pp. 105–145.

HANKS, T. C. 1981. The corner frequency shift, Earth source models, and Q. Bulletin of the Seismological Society of America, **71**, pp. 597–612.

HANKS, T. C., and THATCHER, W. 1972. A graphical representation of seismic source parameters. Journal of Geophysical Research, **77**, pp. 4393–4405.

HANKS, T. C., and WYSS, M. 1972. The use of body-wave spectra in the determination of seismic-source parameters. Bulletin of the Seismological Society of America, **62**, pp. 561–590.

HARTZELL, S. H., and BRUNE, J. 1977. Source parameters for the January 1975 Brawley – Imperial Valley earthquake swarm. Pure and Applied Geophysics, **115**, pp. 333–355.

JOHNSON, L. R., and MCEVILLY, T. V. 1974. Near-field observations and source parameters of central California earthquakes. Bulletin of the Seismological Society of America, **64**, pp. 1855–1886.

KANAMORI, H. 1977. The energy release in great earthquakes. Journal of Geophysical Research, **82**, pp. 2981–2987.

MADARIAGA, R. 1976. Dynamics of an expanding circular fault. Bulletin of the Seismological Society of America, **66**, pp. 639–666.

MARION, G. E., and LONG, L. T. 1980. Microearthquake spectra in the southeastern United States. Bulletin of the Seismological Society of America, **70**, pp. 1037–1054.

MIYATAKE, T. 1980*a*. Numerical simulations of earthquake source process by a three-dimensional crack model. Part I. Rupture process. Journal of Physics of the Earth, **28**, pp. 565–598.

——— 1980*b*. Numerical simulations of earthquake source process by a three-dimensional crack model. Part II. Seismic waves and spectrum. Journal of Physics of the Earth, **28**, pp. 599–616.

NUTTLI, O. 1961. The effect of the Earth's surface on the S wave particle motion. Bulletin of the Seismological Society of America, **51**, pp. 237–246.

OROWAN, E. 1960. Mechanism of seismic faulting. Geological Society of America, Memoir 79, pp. 323–345.

REBOLLAR, C. J., KANASEWICH, E. R., and NYLAND, E. 1982. Focal depths and source parameters of the Rocky Mountain House earthquake swarm from the digital data at Edmonton. Submitted to the Canadian Journal of Earth Sciences.

RICHARDS, T. C., and WALKER, D. J. 1959. Measurements of the thickness of the Earth's crust in the Albertan plains of western Canada. Geophysics, **24**, pp. 262–284.

RUDNICKI, J. W., and KANAMORI, H. 1981. Effects of fault interaction on moment, stress drop, and strain energy release. Journal of Geophysical Research, **86**, pp. 1785–1793.

SAVAGE, J. C. 1974. Relation between P- and S-wave corner frequencies in the spectrum. Bulletin of the Seismological Society of America, **56**, pp. 1621– 1627.

SHAMINA, O. G., PAVLOV, A. A., and STRIZHKOV, S. A. 1978. Model studies of shear displacement along a pre-existing fault. Pure and Applied Geophysics, **116**, pp. 900–912.

THATCHER, W., and HANKS, C. T. 1973. Source parameters of southern California earthquakes. Journal of Geophysical Research, **78**, pp. 8547–8576.

VINOGRADOV, S. D. 1978. Experimental observations of elastic wave radiation characteristics from tensile cracks and pre-existing shear faults. Pure and Applied Geophysics, **116**, pp. 888–899.

WETMILLER, R. J. 1981. Microseismicity in the Rocky Mountain House seismogenic zone, western Canada. Geological Association of Canada – Canadian Geophysical Union (GAC/CGU) Meeting, May, Calgary, Alta., Abstract.

WYSS, M. 1970. Stress estimate for South American shallow and deep earthquakes. Journal of Geophysical Research, **75**, pp. 1529–1544.

WYSS, M., and BRUNE J. N. 1968. Seismic moment, stress, and source dimensions for earthquakes in the California–Nevada region. Journal of Geophysical Research, **73**, pp. 4681–4694.